*Sensors and Materials*, Vol. 28, No. 5 (2016) 539–545
MYU Tokyo



S & M 1207

# Fabrication of Open-End $TiO_2$ Nanotubes Attached to Front-Illuminated Dye-Sensitized Solar Cells

Tung-Lung Wu, Teen-Hang Meen,[1*] Liang-Wen Ji,[**] Shi-Mian Chao,[2]
Chiung-Hsien Huang, Jenn-Kai Tsai,[1] Tien-Chuan Wu,[1] and Chien-Jung Huang[3]

Institute of Electro-Optical and Materials Science, National Formosa University, Yunlin 632, Taiwan
[1]Department of Electronic Engineering, National Formosa University, Yunlin 632, Taiwan
[2]Department of Electrical Engineering, Hsiuping University of Science and Technology, Taichung 412, Taiwan
[3]Department of Applied Physics, National University of Kaohsiung, Kaohsiung 811, Taiwan

(Received August 31, 2015; accepted February 29, 2016)

***Keywords:*** $TiO_2$ nanotubes, front-illuminated, dye-sensitized solar cells

In this study, we used secondary anodization to prepare open-end $TiO_2$ nanotube arrays and then transferred them to fluorine-doped tin oxide (FTO) glass attached to front-illuminated dye-sensitized solar cells (DSSCs). X-ray diffraction (XRD) patterns found that $TiO_2$ nanotubes form the anatase phase when the annealing temperature is greater than 280 °C. The best annealing temperature for $TiO_2$ nanotubes is 450 °C. From field-emission scanning electron microscopy (FE-SEM) analysis, the lengths of $TiO_2$ nanotubes were 15, 21, and 28 μm when anodized for 2, 3, and 4 h, respectively. The conversion efficiency for different lengths of $TiO_2$ nanotube photoelectrodes was 4.82, 5.08, and 4.85% for lengths of 15, 21, and 28 μm, respectively. From the results of electrochemistry impedance spectroscopy (EIS), the value of $R_k$ was 5.4, 5.5, and 5.4 Ω for lengths of $TiO_2$ nanotubes of 15, 21, and 28 μm, respectively. These results indicate that the electron recombination rates for different lengths of $TiO_2$ nanotubes are nearly identical. In addition, the value of $R_d$ ware 8.6, 7.2, and 8.5 Ω for lengths of $TiO_2$ nanotubes of 15, 21, and 28 μm, respectively. This result reveals that overlong $TiO_2$ nanotubes make it difficult for the $I_3^-$ anion to diffuse to the counter electrode, resulting in an increase in diffusion transfer resistance $R_d$ and a decrease in conversion efficiency of the DSSCs. In general, the open-end $TiO_2$ nanotubes attached to front-illuminated DSSCs have a better conversion efficiency for DSSCs than those with back-side illumination, and the best conversion efficiency for DSSCs is 5.08% when the length of the $TiO_2$ nanotubes is 21 μm.

## 1. Introduction

With efficiencies comparable to traditional silicon-based cells, dye-sensitized solar cells (DSSCs) are cost-effective and environmentally friendly, and they have received a great amount of attention lately.[(1)] Granular $TiO_2$ powder is commonly used in DSSC light anode structures. The sol–gel method is used to produce porous film structures, and the small pores form between particles in the transmission path, resulting in greater capacity for dye adsorption and less clutter in the electron transfer path. An overlong path leads to leakage and the probability of electron recombination, thereby affecting the overall conversion efficiency of the solar cells. The $TiO_2$ tubular nanostructure with high surface area and large aspect ratio is beneficial to dye adsorption, and rules of order can

*Corresponding author: e-mail: thmeen@nfu.edu.tw
**Corresponding author: e-mail: lwji@seed.net.tw

ISSN 0914-4935 

be reduced when the electron and the hole have in the transmission probability of recombination. Various methods can be used to synthesize $TiO_2$ nanotubes, such as the hydrothermal method,[2] seeded growth,[3] template-assisted deposition,[4] and anodization.[5] Among these, anodization is a relatively simple method for synthesizing self-organized $TiO_2$ nanotube arrays of large area.[6–9] However, $TiO_2$ nanotubes prepared by anodization, because the growth mode only be used in back-side illumination, resulted in the incident light being partially absorbed by the counter electrode and the electrolyte,[10,11] which in turn diminishes the conversion efficiency of DSSCs.[12–14] Therefore, transparent conductive glass for front-illuminated DSSCs using transferred $TiO_2$ nanotubes is expected to improve photovoltaic performance. In addition, near-ultraviolet (UV) light absorption and front surface light reflection may be caused by having the closed end of the tubes at the bottom of the structure. Removing the barrier layer from the closed bottom is expected to enhance light-harvesting and electron-collecting efficiencies in the photoelectrode. In this study, secondary anodization was used to prepare open-end $TiO_2$ nanotube arrays and to transfer them to fluorine-doped tin oxide (FTO) glass, which was attached to front-illuminated DSSCs. The $TiO_2$ nanotubes and DSSCs were investigated by X-ray diffraction (XRD), field-emission scanning electron microscopy (FE-SEM), current–voltage characteristic analyses, electrochemical impedance spectroscopy (EIS), and incident photon conversion efficiency (IPCE) measurement to study the effects of open-end $TiO_2$ nanotubes on the photoelectrodes of the front-illuminated DSSCs.

## 2. Materials and Methods

### 2.1 Materials

Nanotubes grown on Ti foils (purity of 99.6%, thickness of 0.2 mm) were first anodized by constant current at 60 V in ethylene glycol solution, containing 0.3 wt.% $NH_4F$ and 2 vol.% deionized water at a temperature of 20 °C. The $TiO_2$ nanotubes first anodized were annealed in air at 280 °C for 2 h. The $TiO_2$ nanotubes so prepared were then detached by a second anodization in the same solution for 2 h. After being immersed in 30% $H_2O_2$, the $TiO_2$ nanotubes were detached from the Ti foils and could remove the barrier layer from the closed bottom. A $TiO_2$ paste containing $TiO_2$ nanoparticles (P25) and polyethylene glycol (PEG 20000) was spin-coated onto FTO glass, and the open-end $TiO_2$ nanotubes were immediately transferred onto the paste layers. After dryed in air, the photoelectrodes of the open-end $TiO_2$ nanotubes were annealed in air at 450 °C for 3 h. Pt counter electrodes were coated with a drop of $H_2PtCl_6$ solution and heated at 400 °C for 15 min. To adsorb the N3 dye, the $TiO_2$ nanotubes were immersed in a $3 \times 10^{-4}$ M solution of N3 dye and ethyl alcohol at 50 °C for 12 h in the oven. The working electrodes made of $TiO_2$ nanotubes were then rinsed with ethanol.

### 2.2 Assembling and characterizing the DSSCs

The electrolyte solution was adopted from Ever-light Chemical Industrial Corporation (ESE-20). The electrodes were assembled into a sandwich-type open cell using platinum plate as a counter electrode. Both electrodes were spaced by a polymer film. The thickness of the film was 60 μm, and the size of the $TiO_2$ working electrode was 0.25 $cm^2$ (0.5 × 0.5 $cm^2$). Structural analysis was carried out using XRD. The surface morphology of the samples was observed by FE-SEM. The

UV–vis absorption spectra of the samples were observed using a UV–vis spectrophotometer. The current–voltage and EIS characteristics of the samples were measured using a Keithley 2400 source meter (Keithley Instruments Inc., Cleveland, OH, USA) and were determined under simulated sunlight with white light intensity $P_L$ = 100 mW/cm$^2$. In the IPCE measurement, a xenon lamp (Oriel, model 66150, 75 W) was used as the light source. A chopper and a lock-in amplifier were used for phase-sensitive detection. The IPCE data were collected by shining a monochromatic light on the solar cells with wavelengths from 300 to 800 nm; this was performed using a Keithley 2400 source meter.

## 3. Results and Discussion

Figure 1 shows the XRD patterns of the $TiO_2$ nanotubes. The as-formed $TiO_2$ nanotubes were amorphous and were converted to the anatase phase after annealing. Figure 1(a) shows the XRD pattern of the unannealed $TiO_2$ nanotubes, which does not show the presence of the anatase phase. Figure 1(b) shows the XRD pattern of the $TiO_2$ nanotubes annealed at 280 °C. It is obvious that the $TiO_2$ anatase phase is present. Figure 1(c) shows the XRD pattern of the $TiO_2$ nanotubes annealed at 450 °C. This sample has a better anatase phase than the sample annealed at 280 °C. Therefore the best annealing temperature for the $TiO_2$ nanotubes is 450 °C. Figure 2 shows SEM images of the anodized $TiO_2$ nanotubes under a constant voltage of 60 V with the anodic treatment for 2, 3, and 4 h. The length of the $TiO_2$ nanotubes were 15, 21, and 28 μm for anodization times of 2, 3, and 4 h, respectively. The longer the anodization time, the longer the nanotubes grow. The average growth rate of nanotubes was 7 μm/h. Therefore, the length of the $TiO_2$ nanotubes can be controlled by adjusting the reaction time.

Figure 3 shows the UV–vis absorption spectra for dye adsorbed on different lengths of $TiO_2$ nanotubes. There are two absorption peaks; around 370 and 518 nm. The longest $TiO_2$ nanotubes with a length of 28 μm have better absorption than the shorter ones. This may be due to the longer $TiO_2$ nanotubes having better dye adsorption. Figure 4 shows the IPCE characteristic curves of the

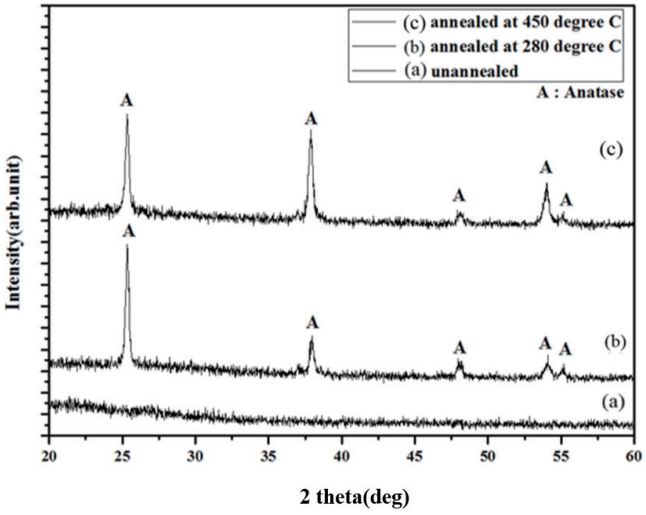


Fig. 1. XRD patterns of $TiO_2$ nanotubes (a) unannealed, (b) annealed at 280 °C, and (c) annealed at 450 °C (A represents the presence of the anatase phase).

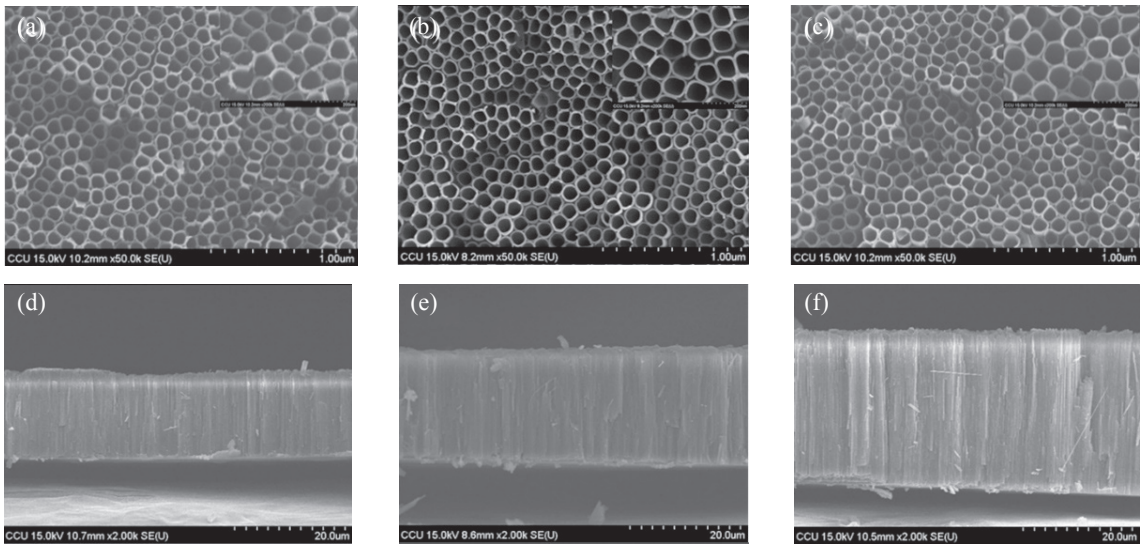


Fig. 2. FE-SEM images of the anodized $TiO_2$ nanotubes under a constant voltage of 60 V with the anodic treatment for (a, d) 2, (b, e) 3, and (c, f) 4 h, and the lengths of $TiO_2$ nanotubes were 15, 21, and 28 μm, respectively.

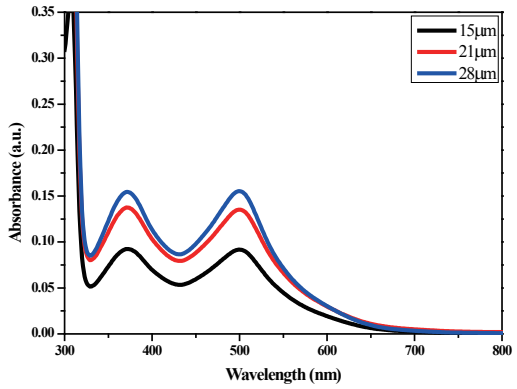


Fig. 3. (Color online) UV–vis absorption spectra for dye adsorbed on different lengths of $TiO_2$ nanotubes.

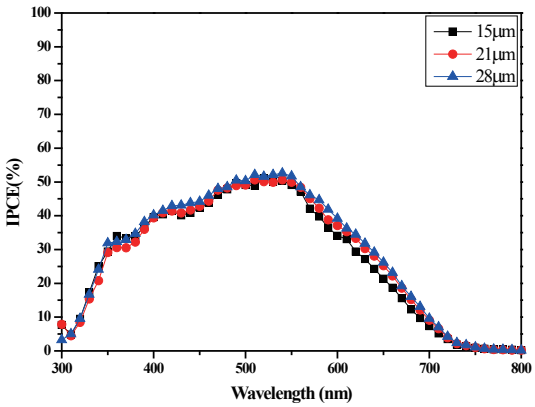


Fig. 4. (Color online) IPCE characteristic curves of the DSSCs with different lengths of $TiO_2$ nanotubes.

DSSCs with different lengths of $TiO_2$ nanotubes. The results of IPCE analysis indicate the number of incident photons inside the cells and their contribution to efficiency. All the IPCE spectra are similar in shape, and the IPCE of the longest $TiO_2$ nanotubes is higher than that of the shorter $TiO_2$ nanotubes, especially from 400 to 700 nm. This may be due to the longer $TiO_2$ nanotubes increasing the partial light incident structure leading to a scattering effect. This also provides evidence for the longer $TiO_2$ nanotubes having better dye adsorption and more incident photons inside the cells than do the shorter nanotubes.

Figure 5 shows the current–voltage characteristics of DSSCs with different lengths of $TiO_2$ nanotubes. The parameters for the short-circuit current density ($J_{sc}$), the open circuit voltage ($V_{oc}$),

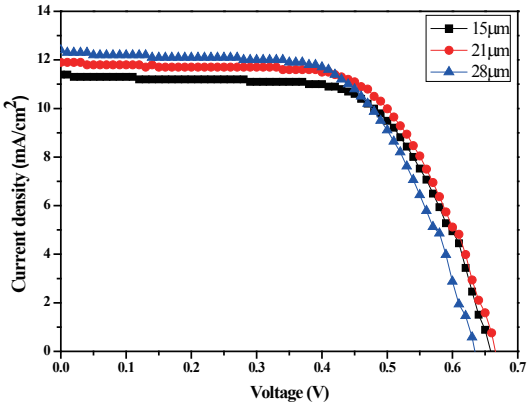


Fig. 5 (Color online) Current–voltage curves for DSSCs with different lengths of $TiO_2$ nanotubes.

Table 1
Parameters of current–voltage characteristics for DSSCs with different lengths of $TiO_2$ nanotubes.

| Length of $TiO_2$ nanotubes (μm) | $V_m$ (V) | $J_m$ (mA/cm²) | $V_{oc}$ (V) | $J_{sc}$ (mA/cm²) | *FF* (%) | $\eta$ (%) |
|---|---|---|---|---|---|---|
| 15 | 0.45 | 10.71 | 0.66 | 11.37 | 64.26 | 4.81 |
| 21 | 0.46 | 11.07 | 0.67 | 11.89 | 63.95 | 5.07 |
| 28 | 0.42 | 11.65 | 0.64 | 12.33 | 62.02 | 4.85 |

the fill factor (*FF*), and the overall conversion efficiency ($\eta$) are listed in Table 1. From the results in Fig. 5 and Table 1, the best conversion efficiency of DSSCs is 5.07% when the length of the $TiO_2$ nanotubes is 21 μm. The conversion efficiency is higher than that for back-illuminated DSSCs.[15–19] The open-circuit voltage decreased from 0.67 to 0.64 V as lengths of nanotubes increased from 21 to 28 μm. This voltage decrease may be due to the $I_3^-$ anion in diffusing to the counter electrode, which in turn leads to a decrease in the reduction reaction and a lower open-circuit voltage.

To study the effect of DSSCs with different lengths of $TiO_2$ nanotubes, the EIS analysis for the $TiO_2$ nanotubes was carried out and the results are shown in Fig. 6. The simulation of the equivalent circuit is discussed in previous reports.[20–22] The parameter $R_k$, which represents charge transfer resistance related to recombination of electrons, is also listed in Table 2. When the length of the $TiO_2$ nanotubes was 15, 21, and 28 μm, the value of $R_k$ was 5.4, 5.5, and 5.4 Ω, respectively, which are almost the same. This result indicates that the electron recombination rate for different lengths of $TiO_2$ nanotubes is nearly the same. In addition, while the length of $TiO_2$ nanotubes increased from 15 to 21 μm, the value of $R_d$, which represents internal diffusion transfer resistance for the electrolyte, decreased from 8.6 to 7.2 Ω. This indicates that more electrons were excited when the length of $TiO_2$ nanotubes increased. However, the value of $R_d$ increased from 7.2 to 8.5 Ω when the length of $TiO_2$ nanotubes increased from 21 to 28 μm. This nesult provides clear evidence that overlong $TiO_2$ nanotubes make diffusion by the $I_3^-$ anion to the counter electrode difficult, resulting in an increase in $R_d$ and a decrease in the conversion efficiency of the DSSCs.

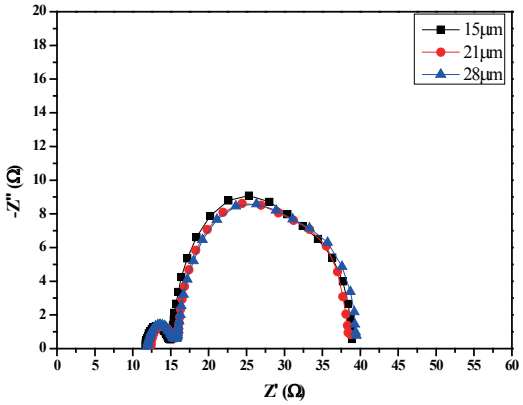


Fig. 6. (Color online) EIS characteristic curves for DSSCs with different lengths of $TiO_2$ nanotubes.

Table 2
Parameters of EIS characteristics for DSSCs with different lengths of $TiO_2$ nanotubes.

| Length of $TiO_2$ nanotubes (μm) | $K_{eff}$ ($s^{-1}$) | $\tau_{eff}$ (s) | $R_s$ (Ω) | $R_{pt}$ (Ω) | $R_k$ (Ω) | $R_d$ (Ω) | $\eta$ (%) |
|---|---|---|---|---|---|---|---|
| 15 | 2.11 | 0.47 | 11.6 | 3.3 | 5.4 | 8.6 | 4.81 |
| 21 | 2.11 | 0.47 | 12.4 | 3.3 | 5.5 | 7.2 | 5.07 |
| 28 | 1.44 | 0.69 | 11.9 | 3.6 | 5.4 | 8.5 | 4.85 |

## 4. Conclusions

In summary, we prepared open-end $TiO_2$ nanotube arrays by secondary anodization for attachment to the photoelectrode of front-illuminated DSSCs. The best conversion efficiency for the DSSCs were 5.08% when the length of $TiO_2$ nanotubes was 21 μm. In general, the open-end $TiO_2$ nanotubes attached to front-illuminated DSSCs have a better conversion efficiency for DSSCs than does the back-side illumination.

## Acknowledgements

This research is supported by the National Science Council, R.O.C., under Contract Nos. MOST 103-2514-S-150-001 and MOST 104-2221-E-150-040.

## References

1 Y. Alivov and Z. Y. Fan: J. Mater. Sci. **45** (2010) 2902.
2 C. C. Tsai and H. S. Teng: Chem. Mater. **16** (2004) 4352.
3 Z. R. R. Tian, J. A. Voigt, J. Liu, B. McKenzie, and H. F. Xu: J. Am. Chem. Soc. **125** (2003) 12384.
4 M. S. Sander, M. J. Cote, W. Gu, B. M. Kile, and C. P. Tripp: Adv. Mater. **16** (2004) 2052.
5 D. Gong, C. A. Grimes, O. K. Varghese, W. C. Hu, R. S. Singh, Z. Chen, and E. C. Dickey: J. Mater. Res. **16** (2001) 3331.
6 G. K. Mor, O. K. Varghese, M. Paulose, N. Mukherjee, and C. A. Grimes: J. Mater. Res. **18** (2003) 2588.
7 J. M. Macak, H. Tsuchiya, and P. Schmuki: Angew. Chem. Int. Ed. **44** (2005) 2100.
8 Y. Yang, X. Wang, and L. Li: Mater. Sci. Eng. B **149** (2008) 58

9 S. Ito, T. N. Murakami, P. Comte, P. Liska, C. Grätzel, M. K. Nazeeruddin, and M. Grätzel: Thin Solid Films **516** (2008) 4613.
10 M. G. Kang, N. G. Park, K. S. Ryu, S. H. Chang, and K. J. Kim: Sol. Energy Mater. & Sol. Cells **90** (2006) 574.
11 S. Ito, N. C. Ha, G. Rothenberger, P. Comte, S. M. Zakeeruddin, P. Pechy, M. K. Nazeeruddin, and M. Grätzel: Chem. Commun. **38** (2006) 4004.
12 D. Zhong, C. Bing, X. Wang, Z. Yang, Y. Xing, S. Miao, W. H. Zhang, and C. Li: Nano Energy **11** (2015) 409.
13 J. Wu, P. Yu, A. S. Susha, K. A. Sablon, H. Chen, Z. Zhou, H. Li, H. Ji, X. Niu, A. O. Govorov, A. L. Rogach, and Z. M. Wang: Nano Energy **13** (2015) 827.
14 X. Y. Dai, C. W. Shi, Y. R. Zhang, and N. Wu: J. Semiconductors **36** (2015) 074003
15 G. K. Mor, K. Shankar, M. Paulose, O. K. Varghese, and C. A. Grimes: Nano Lett. **6** (2006) 215.
16 P. Roy, D. Kim, K. Lee, E. Spiecker, and P. Schmuki: Nanoscale **2** (2010) 45.
17 S. Y. Ho, C. Su, C. C. Cheng, S. Kathirvel, C. Y. Li, and W. R. Li: Nanoscale Res. Lett. **7** (2012) 147.
18 G. Kawamura, H. Ohmi, W. K. Tan, Z. Lockman, H. Muto, and A. Matsuda: Nanoscale Res. Lett. **10** (2015) 219.
19 W. R. Kim, H. Park, and W. Y. Choi: Nanoscale Res. Lett. **10** (2015) 63.
20 R. Kern, R. Sastrawan, J. Ferber, R. Stangl, and J. Luther: Electrochim. Acta **47** (2002) 4213.
21 L. Han, N. Koide, Y. Chiba, A. Islam, and T. Mitate: Comptes Rendus Chimie **9** (2006) 645.
22 M. Adachi, M. Sakamoto, J. Jiu, Y. Ogata, and S. Isoda: J. Phys. Chem. B **110** (2006) 13872.